



# Endogenous Fatty Acids Are Essential Signaling Factors of Pancreatic $\beta$ -Cells and Insulin Secretion

Sebastian Hauke,<sup>1</sup> Kaya Keutler,<sup>1,2</sup> Prasad Phapale,<sup>1</sup> Dmytro A. Yushchenko,<sup>1,3</sup> and Carsten Schultz<sup>1,2</sup>

*Diabetes* 2018;67:1986–1998 | <https://doi.org/10.2337/db17-1215>

**The secretion of insulin from  $\beta$ -cells depends on extracellular factors, in particular glucose and other small molecules, some of which act on G-protein-coupled receptors. Fatty acids (FAs) have been discussed as exogenous secretagogues of insulin for decades, especially after the FA receptor GPR40 (G-protein-coupled receptor 40) was discovered. However, the role of FAs as endogenous signaling factors has not been investigated until now. In the present work, we demonstrate that lowering endogenous FA levels in  $\beta$ -cell medium by stringent washing or by the application of FA-free (FAF) BSA immediately reduced glucose-induced oscillations of cytosolic  $\text{Ca}^{2+}$  ( $[\text{Ca}^{2+}]_i$  oscillations) in MIN6 cells and mouse primary  $\beta$ -cells, as well as insulin secretion. Mass spectrometry confirmed BSA-mediated removal of FAs, with palmitic, stearic, oleic, and elaidic acid being the most abundant species.  $[\text{Ca}^{2+}]_i$  oscillations in MIN6 cells recovered when BSA was replaced by buffer or as FA levels in the supernatant were restored. This was achieved by recombinant lipase-mediated FA liberation from membrane lipids, by the addition of FA-preloaded FAF-BSA, or by the photolysis of cell-impermeant caged FAs. Our combined data support the hypothesis of FAs as essential endogenous signaling factors for  $\beta$ -cell activity and insulin secretion.**

In vertebrates, insulin secretion is a synchronized multicellular process. Sufficiently high blood insulin levels are ensured by the coordinated stimulation of  $\beta$ -cells in pancreatic islets. Coupling of the secretory activity of pancreatic islets results in oscillatory elevations of insulin levels in the bloodstream (1). Studies on patients with diabetes indicate that under oscillatory infusion of insulin, less

insulin is required to sustain normoglycemia compared with a constant insulin supply (2). Disturbed synchronized oscillatory insulin secretion was found in hyperglycemic and hyperinsulinemic *ob/ob* mice and was suggested to contribute to insulin resistance and to the development of type 2 diabetes mellitus (3). The coordination of islets in the pancreas, in addition to gap junctions (4), relies on indirect intercellular communication (i.e., on soluble messengers that reach  $\beta$ -cells by diffusion in the intercellular space of islets and across pancreatic lobes) (5). Individual  $\beta$ -cell activity as well as cell-to-cell coordination in pancreatic islets are predominantly fine-tuned by the close coordination of a multitude of diffusible factors that oscillate in the extracellular space. This includes a number of neurotransmitters and hormones, such as  $\gamma$ -aminobutyric acid (6) and neuropeptide Y (7). In particular,  $\beta$ -cells are equipped with many G-protein-coupled receptors, which are involved in intracellular  $\text{Ca}^{2+}$  signaling and significantly contribute to orchestrating oscillations of the intracellular free  $\text{Ca}^{2+}$  concentration ( $[\text{Ca}^{2+}]_i$  oscillations) and insulin secretion. Examples are purinergic receptors that are triggered by the auto- and paracrine release of ATP from  $\beta$ -cells (8). In 2003, three independent groups reported that GPR40, a G-protein-coupled receptor that is abundantly expressed in the brain and in the pancreas, acts as a receptor for medium- and long-chain fatty acids (FAs) (9–11). GPR40 was found to mediate the majority of the effects that FAs cause on insulin secretion, promoting increased  $[\text{Ca}^{2+}]_i$  (12,13). Deletion of GPR40 expression in pancreatic  $\beta$ -cells led to resistance toward this FA-induced response in  $[\text{Ca}^{2+}]_i$  oscillations and insulin secretion (12,14). GPR40 overexpression, on the other hand, was described to

<sup>1</sup>Cell Biology and Biophysics Unit, European Molecular Biology Laboratory, Heidelberg, Germany

<sup>2</sup>Department of Physiology and Pharmacology, Oregon Health & Science University, Portland, OR

<sup>3</sup>Institute of Organic Chemistry and Biochemistry, Academy of Sciences of Czech Republic, Prague, Czech Republic

Corresponding authors: Carsten Schultz, [schultz@embl.de](mailto:schultz@embl.de), and Dmytro A. Yushchenko, [yushchenko@uochb.cas.cz](mailto:yushchenko@uochb.cas.cz).

Received 6 October 2017 and accepted 2 May 2018.

This article contains Supplementary Data online at <http://diabetes.diabetesjournals.org/lookup/suppl/doi:10.2337/db17-1215/-/DC1>.

© 2018 by the American Diabetes Association. Readers may use this article as long as the work is properly cited, the use is educational and not for profit, and the work is not altered. More information is available at <http://www.diabetesjournals.org/content/license>.

See accompanying article, p. 1932.

augment glucose-stimulated insulin secretion (GSIS) (15), pointing to a major role of GPR40 in FA-stimulated  $[Ca^{2+}]_i$  signaling and GSIS. Recently, we have shown that photo-release of arachidonic acid leads to GPR40 stimulation and subsequent activation of trimeric G-proteins together with  $[Ca^{2+}]_i$  signaling in MIN6 cells (16). For decades, elevated levels of FAs in the bloodstream have been described to significantly augment GSIS in isolated islets (17), animals (18), and nonobese human subjects (19). Studies in rat islets indicate a hypersensitivity of  $\beta$ -cells to glucose after prolonged exposure to FAs (20). In turn, clinical studies correlated artificial decreases of plasma FA levels with the reduction of insulin secretion, indicating an essential role of circulating FAs for efficient GSIS (21,22). Even though FAs have been discussed as insulin secretagogues for decades (as reviewed in Nolan et al. [23]), the role of endogenous FAs in single  $\beta$ -cell activity, intercellular and interislet signaling, and in the synchronization of  $\beta$ -cells has not been investigated so far. In the current study we therefore aimed 1) to determine the role of endogenous FAs as essential endogenous signaling factors for  $\beta$ -cell activity and insulin secretion and 2) to examine whether  $\beta$ -cell activity can be modulated by the removal or replenishment of endogenous FAs. Our approach to subordinate  $\beta$ -cell activity and insulin secretion to the presence of endogenous signaling factors, in particular FAs, contributes to a more detailed and complete understanding of the fundamental regulation of  $\beta$ -cell activity and insulin secretion.

## RESEARCH DESIGN AND METHODS

### Reagents

BSA (FA free [FAF]: catalog #A7030, lot #SLBK9735V; conventional: catalog #A7906, lot #SLBR0420V),  $^{13}C$ -oleic,  $^{13}C$ -palmitic, and  $^{13}C$ -decanoic acid were obtained from Sigma-Aldrich (St. Louis, MO). Thermo Fisher Scientific (Carlsbad, CA) provided gradient-grade Gibco FBS (catalog #16000-044) and DMEM. Solvents were obtained in the highest analytical grade from Biosolve (Valkenswaard, the Netherlands) and Sigma-Aldrich. All other commercially available chemicals and enzymes were purchased from Sigma-Aldrich and Cayman Chemical (Ann Arbor, MI). See Supplementary Data for unit definitions of applied recombinant enzymes.

### Tissue Culture

Insulin-secreting MIN6 cells (24) (passage 25–36) were cultured at 37°C and 8% CO<sub>2</sub> in a humidified atmosphere. MIN6 cells were grown in DMEM containing 4.5 g/L glucose, supplemented with 15% FBS and 70  $\mu$ mol/L  $\beta$ -mercaptoethanol (PAN Biotech, Aidenbach, Germany). MIN6 cells were plated onto eight-well LabTek microscope dishes (catalog #155411; Thermo Fisher Scientific, Rockford, IL), 40-mm coverslips (Menzel Gläser, Braunschweig, Germany) for imaging, or  $\varnothing$  60 mm/ $\varnothing$  35 mm dishes (Nunc Delta Surface, catalog #150288/catalog #153066; Thermo Fisher Scientific, Roskilde, Denmark) to form pseudoislets for in vitro assays.

### Isolation and Culture of Mouse Primary $\beta$ -Cells

Mouse islets were isolated from C57BL/6 mice (female Ctrl:CD1(ICR), outbred (catalog #CD1S1FE07W; Charles River Laboratories) by collagenase digestion, as previously described (25). Briefly, mice were euthanized by cervical dislocation, and a collagenase solution (1 mg/mL) was injected into the bile duct, followed by digestion at 37°C for 10 min and separation of islets using a Histopaque (Sigma-Aldrich) gradient (1.083 and 1.077 g/mL). Islets were cultured in RPMI medium (supplemented with 10% FCS, 100 units/mL penicillin, and 100 mg/mL streptomycin) for 24 h. Upon trypsin digestion (5 min at 37°C), islets were dissociated into single  $\beta$ -cells, which were seeded on poly-L-lysine-coated coverslips. Animals were housed in the European Molecular Biology Laboratory animal facilities under veterinarian supervision and the guidelines of the European Commission (revised directive 2010/63/EU, and American Veterinary Medical Association guidelines 2007).

### Mouse Insulin ELISA

ELISA for the specific quantification of insulin was performed in 96-well format (Merckodia AB, Uppsala, Sweden). Insulin levels were normalized to the protein content of MIN6 cells, using a BCA assay (Pierce BCA Protein assay kit; Thermo Fisher Scientific). Experiments for the determination of supernatant (SN) insulin content were performed in quadruplicate per condition.

### Confocal Laser Scanning Microscopy

Imaging was performed on a FluoView1200 (catalog #IX83; Olympus) confocal laser-scanning microscope at 37°C (incubator box made by the European Molecular Biology Laboratory), using Olympus 60 $\times$  Plan-Apo (numerical aperture 1.4, oil) or 20 $\times$  UPLSAPO (numerical aperture 0.75, air) objectives and FluoView software, version 4.2. The images were acquired with a Hamamatsu C9100-50 EM-CCD camera. The green channel was imaged using a 488-nm laser line (120 mW/cm<sup>2</sup>, 2.5%) and a 525/50 emission mirror. The red channel was imaged using a 559-nm laser (120 mW/cm<sup>2</sup>, 2.0%) and a 643/50 emission filter. Images were acquired in 4-s intervals (frame time 3.9 s). A pulsed 375-nm laser (10 MHz) was applied for uncaging experiments in the entire field of view for eight frames (3.2 s/frame). The dual scanner setup allowed for simultaneous laser stimulation and confocal imaging. This permitted the acquisition of cellular responses that occur during or immediately after laser stimulation. To test changes in  $[Ca^{2+}]_i$  at the single-cell level, MIN6 cells, grown to 70% confluence in pseudoislets, were incubated with an acetoxymethyl ester of the Ca<sup>2+</sup> indicator Fluo-4 (Life Technologies, Eugene, OR), 5  $\mu$ mol/L in DMEM (1 g/L glucose), for 20 min at 37°C. Cell experiments were performed in HEPES buffer (in mmol/L: 115 NaCl, 1.2 CaCl<sub>2</sub>, 1.2 MgCl<sub>2</sub>, 1.2 K<sub>2</sub>HPO<sub>4</sub>, and 20 HEPES, pH 7.4).

### Transfer of Preloaded SN

For  $[Ca^{2+}]_i$  imaging experiments, HEPES buffer (1.5 mL) was preincubated for 30 min on  $2 \times 10^6$  MIN6 cells, grown

to ~80% confluence in  $\varnothing$  60 mm dishes (Thermo Fisher Scientific). One hundred fifty microliters of this SN was transferred to LabTek microscope dishes with prewashed and Fluo-4-stained MIN6 cells residing in 150  $\mu$ L of buffer (1:1 dilution). In dish experiments for the determination of insulin levels, 1.5 mL of SN was transferred to  $2 \times 10^6$  target cells in  $\varnothing$  60 mm dishes (Thermo Fisher Scientific), residing in 1.5 mL of buffer.

#### Perfusion and Static Incubation Experiments

For perfusion experiments, MIN6 cells were seeded on 40-mm glass coverslips and mounted into a Biopetechs FCS2 chamber (chamber volume 0.53 cm<sup>3</sup>,  $\varnothing$  30 mm), connected to a calibrated FCS2 microperfusion pump using Teflon-coated tubing. MIN6 cells were perfused at a constant flow rate of 0.15 mL/min for 30 min. For static incubations, MIN6 cells, prepared in equal densities in  $\varnothing$  30 mm dishes were incubated in buffer for 30 min. Samples were tested for their insulin content (ELISA; Mercodia AB) after respective dilution to equalize differences in volumes. Experiments were performed in the presence of 11 mmol/L glucose.

#### Analysis of Imaging Data

Fluorescence intensities were extracted from individual cells as a function of time using Fiji (26) and were calculated relative to the maximum detected fluorescence intensity after subtraction of background ( $F/F_0$ ). Representative cells within the field of view were averaged to generate  $[Ca^{2+}]_i$  traces or to determine the number of detected high-intensity  $[Ca^{2+}]_i$  events within every 60-s interval. The height of each  $[Ca^{2+}]_i$  event was determined relative to the highest detected peak in each trace as a criterion for grouping  $[Ca^{2+}]_i$  transients into high-intensity events ( $\geq 60\%$  of highest peak) and low-intensity events ( $< 60\%$  of highest peak). For statistical analysis, four to six independent experiments were performed per condition. At least 30 individual MIN6 cells or 60 mouse primary  $\beta$ -cells showing representative behavior were picked per condition, and their responses were averaged.

#### Fluorescence Displacement Assay

A solution of Nile red 2-*O*-butyric acid (NRBA) and FAF-BSA (10  $\mu$ mol/L) in a 1:1 ratio was preincubated at 37°C for 20 min. NRBA preferably binds hydrophobic protein domains along with a turn-on of fluorescence emission and a strong shift to shorter wavelengths (27). Buffer (11 mmol/L glucose) was incubated on  $2 \times 10^6$  MIN6 cells, allowing for the accumulation of FAs. The FA-containing buffer was concentrated to 10% of its original volume using a concentrator (catalog #7310032; Labconco, Fort Scott, KS) and added to NRBA-loaded FAF-BSA. Assays were performed on a QuantaMaster QM4/2000SE Photon Technology International spectrofluorometer in 150- $\mu$ L quartz cuvettes. After excitation at  $\lambda = 540$  nm, full emission scans were recorded ( $\lambda = 550$ –750 nm) with 2-nm step intervals and 0.2-s integration time.

#### Preparation of Biological Samples for the Extraction of FAs

A total of  $1 \times 10^6$  MIN6 cells were seeded to form pseudoislets in 60-mm dishes within 5 days. MIN6 cells were prestimulated with buffer (11 mmol/L glucose) for 30 min at 37°C. A total of 1.6 mL of buffer (supplemented with BSA, 11 mmol/L glucose) was incubated on MIN6 cells for 20 min at 37°C. A total of 1.5 mL of the SN was concentrated to 120  $\mu$ L at 4°C using a concentrator (catalog #7310032; Labconco). MIN6 cells were scraped in 120  $\mu$ L of buffer.

#### FA Extraction

FAs were extracted using an MeOH/CHCl<sub>3</sub> extraction procedure at 4°C, according to Clark et al. (28). Seven hundred fifty microliters of mix A (4.48 mL of MeOH, 2.42 mL of CHCl<sub>3</sub>, and 0.236 mL of HCl [1 N]) were added to biological samples, which were vortexed for 30 s. Thirty microliters of MeOH, containing the internal standards <sup>13</sup>C-palmitic acid (100 ng/sample), <sup>13</sup>C-oleic acid (OA) (50 ng/sample), and <sup>13</sup>C-decanoic acid (25 ng/sample) were added per sample. Seven hundred twenty-five microliters of CHCl<sub>3</sub> and 170  $\mu$ L of 2 mol/L HCl were added, followed by vortexing for 30 s. Samples were centrifuged at 8,000g (10 min, 4°C) to create a two-phase system with an upper aqueous layer and a protein band at the interface. The lower organic phase was collected in a fresh tube. Seven hundred eight microliters of mix B (7.2 mL of CHCl<sub>3</sub>, 3.6 mL of MeOH, and 2.7 mL of 0.01 mol/L HCl) were added to the lower phase. Samples were mixed and centrifuged (8,000g, 10 min, 4°C). The upper phase was removed, and the samples were dried at 4°C using a concentrator (catalog #7310032; Labconco). All applied materials were pretreated with methanol to eliminate possible palmitate contaminations, according to Yao et al. (29).

#### Liquid Chromatography Mass Spectrometry

Liquid chromatography-tandem mass spectrometry (MS) analysis was performed on a Vanquish UHPLC System (Thermo Fisher Scientific, Waltham, MA), coupled to a Q-Exactive Plus high-resolution mass spectrometer (Thermo Fisher Scientific) in electrospray ionization-negative mode. The separation of FAs was carried out on an Agilent Poroshell column (3  $\times$  50 mm; 2.7  $\mu$ m) at 0.26 mL/min and 40°C. The mobile phase consisted of solvents A (acetonitrile/water 6:4) and B (isopropyl alcohol/acetonitrile 9:1), buffered with 10 mmol/L ammonium acetate. The Vanquish UHPLC System was set up in gradient mode (Supplementary Table 1). FAs were detected with a full high-resolution mass spectrometer scan at the mass resolving power  $R = 70,000$  in a mass range of 100–1,200  $m/z$ . Data-dependent tandem MS scans were obtained along with full scans using higher-energy collisional dissociation with normalized collision energies of 10, 20, and 30 units at the mass resolving power  $R = 17,500$ . See Supplementary Data for details.

## RESULTS

Removal and Replenishment of Endogenous Signaling Factors Modulate the Levels of Cytosolic  $[Ca^{2+}]_i$  and Insulin Secretion

It is well established that static incubation of MIN6 cells in the presence of glucose (11 mmol/L) is characterized by periodic transients of cytosolic  $[Ca^{2+}]_i$  ( $[Ca^{2+}]_i$  oscillations) (Fig. 1A*i* and B*i*). In accordance with literature data, MIN6 cells respond to elevated glucose levels by  $[Ca^{2+}]_i$  oscillations

and increased insulin secretion, similar to mouse primary  $\beta$ -cells (Supplementary Fig. 1) (30). Because  $[Ca^{2+}]_i$  oscillations correlate with insulin secretion (Supplementary Fig. 1) (31–33), they may serve as a sensitive readout of  $\beta$ -cell responses.  $[Ca^{2+}]_i$  oscillations can be followed in real time, using  $Ca^{2+}$ -sensitive cell-permeant fluorescent indicators, such as Fluo-4 (34). We observed that extensive perfusion (1.5 mL/min for 1 min) of MIN6 cells with buffer containing 11 mmol/L glucose paused  $[Ca^{2+}]_i$  oscillations,

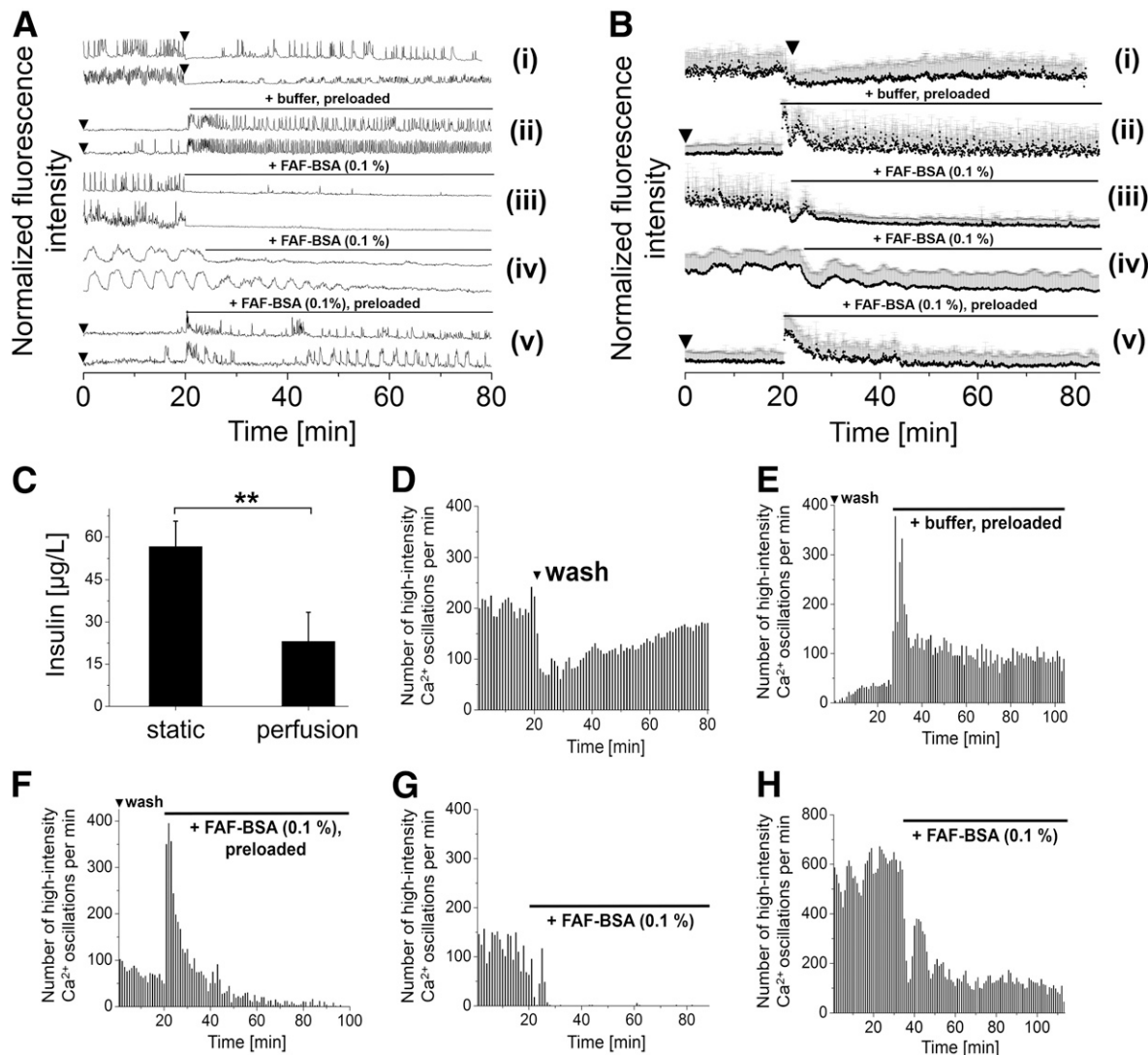


**Figure 1**—Essential role of endogenous signaling factors for  $\beta$ -cell activity and insulin secretion. Representative single (A) and averaged (B) calcium traces from MIN6 cells and mouse primary  $\beta$ -cells, recorded with the  $Ca^{2+}$  indicator Fluo-4. Trace *i*: Stringent washing of MIN6 cells (1.5 mL/min, black arrows) reduced  $[Ca^{2+}]_i$  oscillations, which recovered during the following static incubation. Trace *ii*: Transfer of preloaded buffer to washed MIN6 cells immediately recovered  $[Ca^{2+}]_i$  oscillations. Addition of FAF-BSA (0.1%) to MIN6 cells (trace *iii*) and mouse primary  $\beta$ -cells (trace *iv*) significantly reduced or terminated  $[Ca^{2+}]_i$  oscillations. Trace *v*: Transfer of  $\beta$ -cell SN with BSA (0.1%) preloaded on  $2 \times 10^6$  MIN6 cells (30-min loading time) to washed MIN6 cells restarted  $[Ca^{2+}]_i$  oscillations. C: Constant perfusion of MIN6 cells reduced insulin secretion by  $\sim 60\%$ , compared with static incubation. Experiments for the determination of insulin levels were performed in quadruplicate. D–H: Number of detected high-intensity  $[Ca^{2+}]_i$  events within every 60-s interval. Recovery of  $[Ca^{2+}]_i$  oscillations after stringent perfusion (D) and after washing (E), upon the addition of SN (buffer preincubated with MIN6 cells) or FAF-BSA (0.1%) (F) that was preloaded on MIN6 cells. Reduction of  $[Ca^{2+}]_i$  oscillations in MIN6 cells (G) and mouse primary  $\beta$ -cells (H) after the addition of FAF-BSA (0.1%). Shown are averages of  $n = 30$  MIN6 cells and  $n = 60$  mouse primary  $\beta$ -cells.  $**P < 0.01$ , ANOVA. Error bars represent the SD. See Supplementary Fig. 2 for the setup of the perfusion system and Supplementary Fig. 3 for exemplary single  $Ca^{2+}$  traces. Experiments were conducted in the presence of glucose (11 mmol/L).

which gradually recovered only after the termination of perfusion (Fig. 1Ai, Bi, and D). Similar effects were observed upon washing MIN6 cells and mouse primary  $\beta$ -cells in the microscopy dish before imaging (Fig. 1Aii, Bii, Av, and Bv). In line with this observation, constant perfusion (0.15 mL/min) of MIN6 cells significantly reduced insulin secretion, compared with static incubation (Fig. 1C), suggesting that stringent washing removed components from the extracellular space that are necessary for GSIS. In an attempt to verify whether endogenous signaling factors, secreted by  $\beta$ -cells, are modulating GSIS, we preincubated a population of  $2 \times 10^6$  MIN6 cells with buffer for 30 min (i.e., SN) and transferred this SN to a dish with freshly washed MIN6 cells. Such a buffer exchange led to an immediate and full recovery of  $[Ca^{2+}]_i$  oscillations in all MIN6 cells (Fig. 1Aii, Bii, and E) and enhanced insulin secretion (Supplementary Fig. 4), and was observed for all tested SNs at various glucose concentrations (Supplementary Fig. 5). SNs generated from HeLa cells under identical conditions restarted  $[Ca^{2+}]_i$  oscillations only in 3 of 100 MIN6 cells, but did not change insulin secretion (Supplementary Fig. 4).

#### BSA-Mediated Buffering of FA Levels Modulates $\beta$ -Cell Activity

Guided by our results from the photolysis of arachidonic acid in MIN6 cells (16), we decided to examine the effect of FA depletion on  $[Ca^{2+}]_i$  oscillations and insulin secretion. Depletion of FAs in cell medium was achieved by adding FAF-BSA to MIN6 cells cultured with 11 mmol/L glucose (see the MS analysis below for quantification, Fig. 4). The addition of 1% and 0.1% FAF-BSA to the medium led to immediate termination of  $[Ca^{2+}]_i$  oscillations in MIN6 cells and in mouse primary  $\beta$ -cells (Fig. 1Aiii, Biii, Aiv, Biv, G, and H and Supplementary Figs. 6, 7, and 8, Supplementary Movie 1), whereas the addition of 0.01% FAF-BSA had a weak to no effect (Supplementary Fig. 9). In the presence of 0.1% FAF-BSA, the levels of secreted insulin decreased by  $>80\%$  (Fig. 2H). The exchange of FAF-BSA to BSA-free buffer led to slow ( $\sim 20$ – $30$  min) recovery of  $[Ca^{2+}]_i$  oscillations in the case of 1% FAF-BSA and close to immediate recovery in the case of 0.1% and 0.01% FAF-BSA (Fig. 2Ai, Bi, and C and Supplementary Figs. 6, 7, and 9). The effects of BSA on  $[Ca^{2+}]_i$  oscillations were readily reproduced using human serum albumin (see Supplementary Fig. 10) and were independent of the glucose levels that were applied (Supplementary Fig. 11). The addition of conventional BSA (i.e., BSA saturated by natural FA cargo) (Fig. 4C, mass spectrometric analysis) to MIN6 cells and mouse primary  $\beta$ -cells in 0.1% (and 1%) final concentrations did not show pronounced effects on  $[Ca^{2+}]_i$  oscillations (Fig. 2Aii, Bii, Aiii, Biii, D, and E and Supplementary Figs. 6 and 7). Furthermore, FAF-BSA, presaturated with the BSA binders L-tryptophan (L-Trp) (35) or ibuprofen (Ibu) (36) exhibited much weaker effects on  $[Ca^{2+}]_i$  oscillations in MIN6 cells and mouse primary  $\beta$ -cells than FAF-BSA alone (Fig. 2Aiv–vi, Biv–vi, F, and G and Supplementary Figs. 6 and 7), indicating

that BSA with a low capacity to extract FAs does not significantly affect  $[Ca^{2+}]_i$  oscillations.

The addition of FAF-BSA, preloaded by incubation on  $2 \times 10^6$  MIN6 cells, to prewashed MIN6 cells immediately resumed  $[Ca^{2+}]_i$  oscillations (Fig. 1Av, Bv, and F), indicating that BSA was saturated with cargo that was readily off-loaded again. The recovery of  $[Ca^{2+}]_i$  oscillations directly correlated with the preloading time of FAF-BSA on MIN6 cells and therefore presumably with the total amount of transferred FAs. Consistently, increased responses were observed for higher concentrations (5%) of BSA preloaded on MIN6 cells for the same preloading time (Supplementary Fig. 12). The addition of Ibu or L-Trp (400  $\mu$ mol/L) to MIN6 cells in the presence of BSA preloaded on MIN6 cells also augmented  $[Ca^{2+}]_i$  oscillations. This points to a stimulation of MIN6 cells caused by FAs that were released from BSA because of out-competition by Ibu or L-Trp (Supplementary Fig. 13). In order to verify whether FAs are actually the major cargo in BSA transfer experiments, the GPR40 inhibitor GW1100 (10  $\mu$ mol/L) (37) was added together with FAF-BSA (1%, preloaded on MIN6 cells) to prewashed MIN6 cells. This led to one prominent  $[Ca^{2+}]_i$  spike followed by the suppression of continuous  $[Ca^{2+}]_i$  oscillations (Fig. 3Ai, Bi, and C). This suggests that that GPR40 activation is crucial for inducing  $[Ca^{2+}]_i$  oscillations in glucose-stimulated MIN6 cells, in accordance with the findings of Schnell et al. (12). In line with this, GW1100-treated MIN6 cells showed a significant decrease (10  $\mu$ mol/L) or termination (25  $\mu$ mol/L) of  $[Ca^{2+}]_i$  oscillations, possibly because of competition with endogenous FAs for GPR40 (Fig. 3Aiii, Biii, E, and F and Supplementary Fig. 14).

#### Mass Spectrometry Reveals BSA-Mediated Extraction of FAs From MIN6 Cells

We turned to MS to demonstrate the enrichment of FAs upon incubation of FAF-BSA on MIN6 cells. We used 0.1% FAF-BSA, because this concentration was shown to immediately terminate  $[Ca^{2+}]_i$  oscillations in MIN6 cells. All materials were cleaned with methanol to avoid palmitic acid contamination, according to Yao et al. (29). SNs were subjected to chloroform/methanol extraction, followed by MS analysis. Palmitic acid and stearic acid (SA) were detected as the most prominent FAs in MIN6 cell SNs (Fig. 4A), which supports the hypothesis that FAs serve as endogenous signaling factors. Incubation of MIN6 cells with 0.1% FAF-BSA increased the detected levels of oleic, elaidic, and SA 38-, 57-, and 29-fold (Fig. 4A). The occurrence of FAs in FAF-BSA preloaded on MIN6 cells was similar to FAs obtained from MIN6 cell extracts. In cell extracts, stearic, palmitic, arachidonic, oleic, and elaidic acid were the most abundant (Fig. 4B). These data support the hypothesis that FAF-BSA treatment is an effective approach for capturing FAs from MIN6 cells. As expected from  $[Ca^{2+}]_i$  imaging, conventional BSA was found to be loaded with considerable amounts of FAs even before incubation on MIN6 cells, explaining its reduced capacity to capture FAs from MIN6 cell SNs (Fig. 4C).

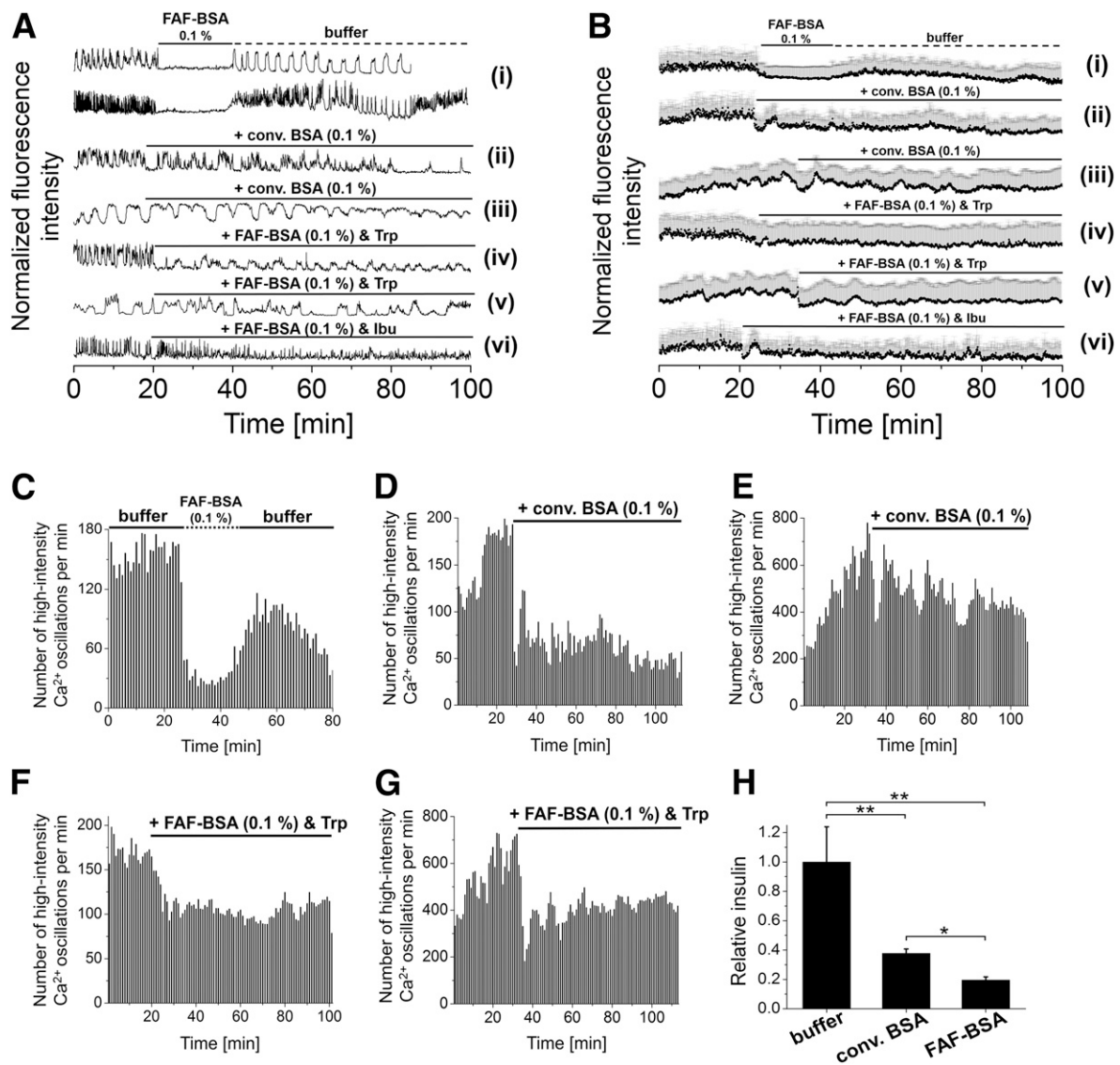


**Figure 2**—Modulation of  $\beta$ -cell  $[\text{Ca}^{2+}]_i$  oscillations by BSA. Representative single (A) and averaged (B) calcium traces from MIN6 cells and mouse primary  $\beta$ -cells, recorded with the  $\text{Ca}^{2+}$  indicator Fluo-4. Trace i: Addition of FAF-BSA (0.1%) to glucose-stimulated MIN6 cells immediately terminated  $[\text{Ca}^{2+}]_i$  oscillations. Oscillations resumed when FAF-BSA was exchanged by buffer. Addition of conventional (conv.) BSA (0.1%) or FAF-BSA (0.1%) that was presaturated with L-Trp (Trp) or Ibu to MIN6 cells (traces ii, iv, and vi) or mouse primary  $\beta$ -cells (traces iii and v) reduced, but did not stop,  $[\text{Ca}^{2+}]_i$  oscillations. C–G: Number of detected high-intensity  $\text{Ca}^{2+}$  events within every 60-s interval. C: Decrease and recovery of  $[\text{Ca}^{2+}]_i$  oscillations after the addition of FAF-BSA (0.1%) and replacement by buffer. Decrease of  $[\text{Ca}^{2+}]_i$  oscillations after addition of conv. BSA (0.1%) to MIN6 cells (D) or mouse primary  $\beta$ -cells (E). Trp-presaturated FAF-BSA (0.1%) reduced, but did not terminate,  $[\text{Ca}^{2+}]_i$  oscillations in MIN6 cells (F) and mouse primary  $\beta$ -cells (G). H: FAF-BSA (0.1%) reduced insulin secretion from MIN6 cells by >80% compared with BSA-free buffer. Experiments for the determination of insulin levels were performed in quadruplicate. For imaging, averages of  $n = 30$  MIN6 cells and  $n = 60$  mouse primary  $\beta$ -cells are shown.  $**P < 0.01$ ;  $*P < 0.05$ , ANOVA. Error bars represent the SD. See Supplementary Fig. 6 for exemplary single  $\text{Ca}^{2+}$  traces and Supplementary Fig. 15 for technical details of insulin quantification in the presence of BSA. Experiments were conducted in the presence of glucose (11 mmol/L).

FA levels in the SNs of MIN6 cells, as revealed by MS, were confirmed by a fluorescence displacement assay, based on the environmentally sensitive fluorophore NRBA (38). Fluorescence emission from BSA-bound NRBA dropped in the presence of MIN6 cell SNs, depending on the preincubation time of the SNs on MIN6 cells (Fig. 5A). This detected incubation time dependence underlines the important role of FAs as endogenous signaling factors for MIN6 cells.

#### Replenishing FA Levels at the Plasma Membrane of MIN6 and Mouse Primary $\beta$ -Cells Restarts $[\text{Ca}^{2+}]_i$ Oscillations in FAF-BSA-Treated $\beta$ -Cells

The previously described results indicated that lowering endogenous FA levels was the major cause of the observed termination of  $[\text{Ca}^{2+}]_i$  oscillations and the depletion of insulin secretion in FAF-BSA-treated MIN6 cells and mouse primary  $\beta$ -cells. In order to verify whether replenishing extracellular FA pools would restart  $[\text{Ca}^{2+}]_i$

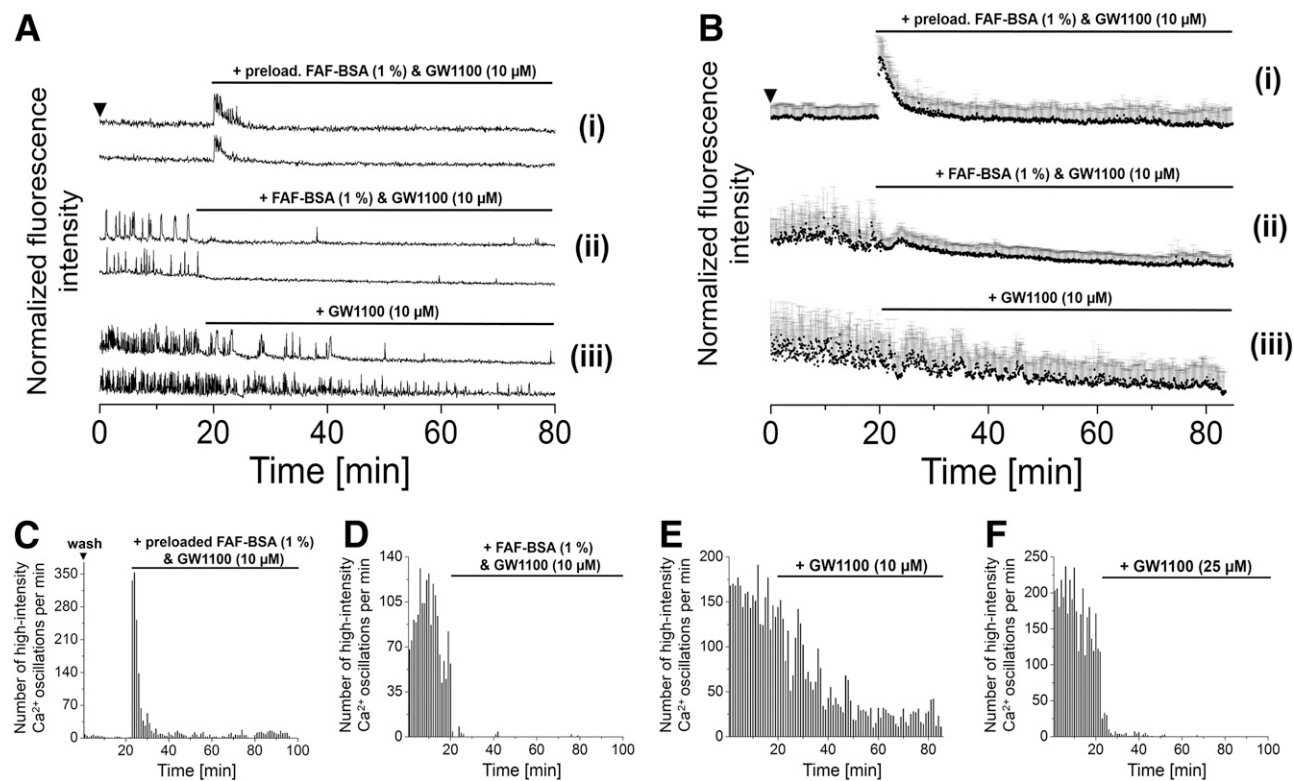


**Figure 3**—Transfer of FAs stimulates  $[Ca^{2+}]_i$  oscillations via GPR40. Representative single (A) and averaged (B)  $Ca^{2+}$  traces from MIN6 cells were recorded with the  $Ca^{2+}$  indicator Fluo-4. Trace i: The GPR40 inhibitor GW1100 (10  $\mu$ mol/L) was spiked to FAF-BSA (1%) that was preloaded on MIN6 cells (30-min preloading on  $2 \times 10^6$  cells), leading to a single, but prominent,  $[Ca^{2+}]_i$  transient without evoking continuous  $[Ca^{2+}]_i$  oscillations. Trace ii: FAF-BSA (1%, no preloading) spiked with GW1100 (10  $\mu$ mol/L) terminated  $[Ca^{2+}]_i$  oscillations. Trace iii: GW1100 (10  $\mu$ mol/L) gradually decreased  $[Ca^{2+}]_i$  oscillations in MIN6 cells. C–F: Number of detected high-intensity  $[Ca^{2+}]_i$  events within every 60-s interval. C: MIN6 cells preloaded BSA (+GW1100, 10  $\mu$ mol/L) induced a prominent  $[Ca^{2+}]_i$  transient upon the addition to prewashed MIN6 cells, without evoking continuous  $[Ca^{2+}]_i$  oscillations. D: Addition of FAF-BSA (1% +GW1100, 10  $\mu$ mol/L) terminated  $[Ca^{2+}]_i$  oscillations. E: GW1100 (10  $\mu$ mol/L) gradually decreased  $[Ca^{2+}]_i$  oscillations. F: This effect was enhanced when 25  $\mu$ mol/L GW1100 was applied. Shown are averages of  $n = 30$  MIN6 cells and  $n = 60$  mouse primary  $\beta$ -cells. Error bars represent the SD. See Supplementary Fig. 12 for exemplary single  $Ca^{2+}$  traces. Experiments were conducted in the presence of glucose (11 mmol/L).

oscillations, we used sulfo-caged (Scg) FAs bearing a photolabile negatively charged caging group to allow quantitative delivery and localization of Scg-FA exclusively at the plasma membrane (PM) (Fig. 5D). Based on our findings from MS (Fig. 4) and our previous results (16), we applied Scg-SA and Scg-OA. Because of the fluorescence of the coumarin cage, BSA-mediated depletion of Scg-SA from MIN6 cells could be directly monitored by fluorescence microscopy. The addition of FAF-BSA to Scg-SA-loaded MIN6 cells significantly diminished the fluorescent signal at the PM within seconds (Fig. 5C and D). Furthermore, the fluorescence signal inversely correlated with the applied FAF-BSA concentration, indicating that the Scg-FA was efficiently extracted by FAF-BSA from PMs (Fig. 5B), leading to the termination of  $[Ca^{2+}]_i$  oscillations. In line with our previous work, subsequent illumination of Scg-FA-loaded MIN6 cells with ultraviolet (UV) light permitted the release of FA with good spatiotemporal control (16). When applied to MIN6 cells and mouse primary  $\beta$ -cells, pretreated with FAF-BSA (0.1%), UV-mediated liberation of SA from Scg-SA (200  $\mu$ mol/L) (Fig. 6Ai, Bi, Aii, Bii, C,

and D) resulted in immediate resumption of  $[Ca^{2+}]_i$  oscillations. Comparable effects were observed for Scg-OA (Supplementary Fig. 17). Less controlled replenishment of FAs by the simple addition of OA (200  $\mu$ mol/L) to FAF-BSA (0.1%)-treated MIN6 cells and mouse primary  $\beta$ -cells also recovered  $[Ca^{2+}]_i$  oscillations (Fig. 6Aiii, Biii, Aiv, Biv, E, and F). These observations indicate that endogenous FAs not only are essential, but provide a sufficient signal to induce  $[Ca^{2+}]_i$  oscillations in glucose-stimulated  $\beta$ -cells.

#### Modulating $\beta$ -Cell Activity by Enzyme-Mediated FA Liberation

As an alternative way to artificially elevate extracellular FA levels after FAF-BSA treatment, we used recombinant lipases. Phospholipase A<sub>2</sub> (PLA<sub>2</sub>) is known to liberate FAs from membrane lipids by the hydrolysis of zwitterionic glycerophospholipids (39). Upon the addition of recombinant PLA<sub>2</sub> (10 units),  $[Ca^{2+}]_i$  oscillations in MIN6 cells and mouse primary  $\beta$ -cells increased. The induced oscillations were terminated by the addition of 1% FAF-BSA (Fig. 7Ai–iii, Bi–iii, D, and E). Similar effects were observed for recombinant

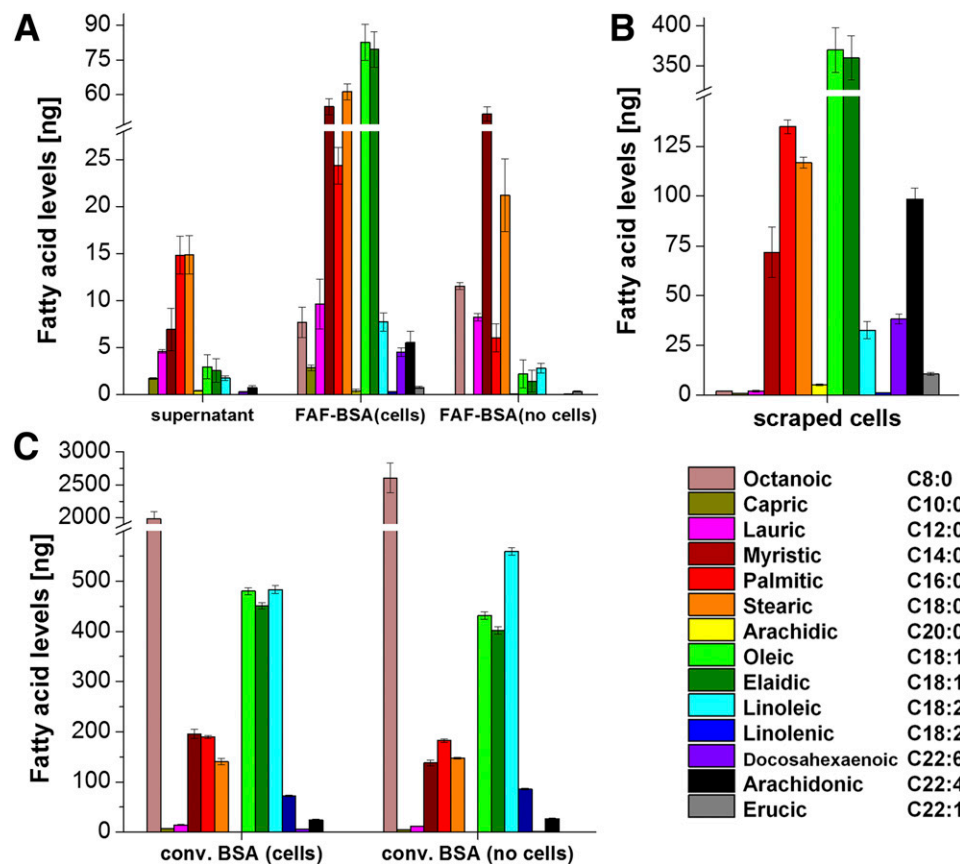


**Figure 4**—Mass spectrometric analysis of BSA-mediated FA extraction from MIN6 cells. **A:** FA levels, obtained from MIN6 cell SNs, from FAF-BSA (0.1%) after incubation on MIN6 cells (cells) or from FAF-BSA (0.1%) that was not added to cells (no cells). Palmitic acid and SA were the most abundant FAs in MIN6 cell SN. FAF-BSA (0.1%) incubated with MIN6 cells was enriched in OA, elaidic acid, SA, and palmitic acid. **B:** Levels of different FAs obtained upon extraction of scraped MIN6 cells. **C:** Conventional (conv.) BSA contained considerable amounts of BSA-bound FAs before the incubation on MIN6 cells. Each experiment was conducted with  $2 \times 10^6$  MIN6 cells. Measurements were performed in quadruplicate. Error bars represent the SD. Experiments were performed in the presence of 11 mmol/L glucose.

lipoprotein lipase (500 units), an enzyme that hydrolyzes triglycerides to FAs and glycerol (40) (Fig. 5Aiv, Biv, and F). Removal of PLA<sub>2</sub> from MIN6 cells via buffer exchange diminished induced [Ca<sup>2+</sup>]<sub>i</sub> oscillations (Fig. 7Aii). The presence of recombinant PLA<sub>2</sub> on MIN6 cells increased insulin levels more than sevenfold (Fig. 7C). The inhibition of endogenous PLA<sub>2</sub> by methyl arachidonyl fluorophosphate (MAF) (10 μmol/L) or bromoenol lactone (BEL) (10 μmol/L) decreased and eventually terminated [Ca<sup>2+</sup>]<sub>i</sub> oscillations in MIN6 cells and mouse primary β-cells (Fig. 7Av–vii, Bv–vii, G, and H) and insulin secretion from MIN6 cells (Fig. 7C). Our results demonstrate that elevated FA levels stimulate [Ca<sup>2+</sup>]<sub>i</sub> oscillations and insulin secretion, independent of the origin of FAs. This effect was counteracted by the buffering capacity of albumins.

## DISCUSSION

Previous studies in the field have focused on exogenous FAs as major secretagogues for nutrient-modulated release of adequate amounts of insulin (41,42). To the best of our knowledge, the essential role of endogenous FAs in intercellular pancreatic signaling for insulin secretion has not

been demonstrated so far. To address this topic, we chose the insulinoma cell line MIN6 as a highly relevant model system of pancreatic β-cells. As has been previously shown, MIN6 cells and mouse primary β-cells exhibit very similar signaling patterns for the regulation of insulin secretion (30,43). Key results obtained from MIN6 cells were validated in mouse primary β-cells. Monitoring intracellular [Ca<sup>2+</sup>]<sub>i</sub> oscillations allowed the sensitive assessment of individual β-cell responses on a single-cell level, while ELISA tests served for the quantification of bulk changes in insulin secretion in response to FAF-BSA treatment and variation of FA levels.

The objectives of this study were to examine the essential roles of endogenous FA signaling in basal β-cell activity and insulin secretion. To resemble physiological conditions, we applied serum albumin in FA-stripped and FA-loaded forms to MIN6 cells and mouse primary β-cells. Albumins are well known to bind FAs (44). We found that stringent washing of MIN6 cells and mouse primary β-cells or the application of serum albumins immediately terminated [Ca<sup>2+</sup>]<sub>i</sub> oscillations and diminished insulin secretion. Hence, FAs seemed likely to belong to the secreted components that activate β-cells and are readily captured



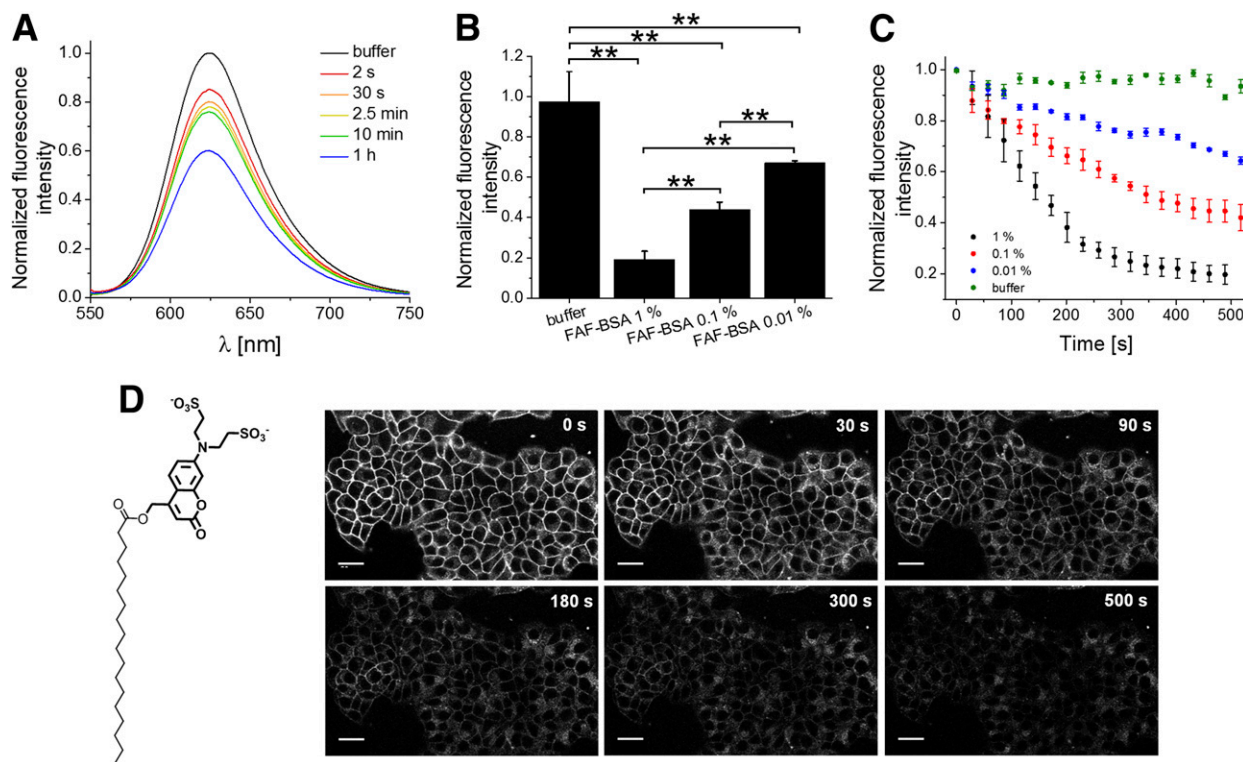


**Figure 5**—Monitoring BSA-mediated extraction of FAs from MIN6 cells, based on a fluorescent displacement assay and Scg-SA coumarin fluorescence. **A**: NRBA-based fluorescence displacement assay for monitoring the levels of FAs in SNs of MIN6 cells. Buffer was preloaded on  $2 \times 10^6$  MIN6 cells for the indicated periods of time and incubated with FAF-BSA, preloaded with NRBA. Outcompetition by FAs, along with a decrease of fluorescence intensity provided quantification of the FA load in the SN. The buffer value (without MIN6 cells, black) served as a reference for normalization. Measurements were performed in quadruplicate per time point. **B** and **C**: Quantification of FAF-BSA-mediated extraction of Scg-SA (200  $\mu\text{mol/L}$ ) from MIN6 cell PMs based on the fluorescence of the sulfo-coumarin cage. The fluorescence intensity was normalized to the signal prior to FAF-BSA (buffer) addition. For each condition, 100–150 MIN6 cells were averaged.  $**P < 0.01$ , ANOVA. Error bars represent the SD. **D**: Structure of Scg-SA and sample images of MIN6 cells, pretreated with Scg-SA (200  $\mu\text{mol/L}$ ), in the presence of FAF-BSA (1%) for the indicated periods. Scale bars, 20  $\mu\text{m}$ . Experiments were conducted in the presence of 11 mmol/L glucose.

by FA-stripped serum albumin from PMs. This suggested that there are adequate FAs in PMs, which was supported by MS analysis. Compared with conventional BSA, the FA content of FAF-BSA was found to be  $\sim 30$  times lower, which indicated that FAF-BSA was significantly depleted in FAs and had a considerable capacity for the withdrawal of FAs from PMs. We observed that FAF-BSA preferentially binds saturated and monounsaturated long-chain FAs (C16–C20/22), such as OA, elaidic acid, SA, and palmitic acid. This is in line with reports in the literature, according to which FAF-BSA preferentially binds medium- and long-chain FAs (44,45). Indeed, the incubation of FAF-BSA on MIN6 cells led to a threefold increase in the levels of BSA-bound SA. In contrast, the levels of BSA-bound OA and elaidic acid increased by a factor of  $\sim 18$ . Decreased  $[\text{Ca}^{2+}]_i$  oscillations in MIN6 cells incubated with FAF-BSA swiftly recovered after uncaging of Scg-SA and Scg-OA or by the addition of OA. This indicates that  $[\text{Ca}^{2+}]_i$  do not depend on a particular long-chain FA species, but can be induced by different long-chain FAs. Despite the fact that fluorescent Scg-FAs are not identical to natural FAs, we showed that they are readily extracted

from the PM by the addition of FAF-BSA in different concentrations. In line with this result,  $[\text{Ca}^{2+}]_i$  oscillations were stimulated by serum albumin-mediated off-loading of FAs, underlining their essential regulating role for  $\beta$ -cell activity and their physiological relevance under different nutritional conditions. Although the addition of FA-stripped serum albumin immediately terminated  $[\text{Ca}^{2+}]_i$  oscillations, the effect was less dramatic in the presence of competing ligands, such as L-Trp or Ibu. FAs were shown to bind to albumin pockets I–III. Interestingly, site II has also been described as a discrete binding site for certain drugs and Trp (35,46,47). The occupation of albumin sites by L-Trp, Ibu, or preliminary FA loading (for conventional BSA, as shown by MS) might have reduced the FA loading capacity, leading to the weaker effects on  $[\text{Ca}^{2+}]_i$  oscillations. Out-competition or cooperative effects at albumin binding sites provide an explanation for the observed stimulation of  $[\text{Ca}^{2+}]_i$  oscillations in competition experiments, when Trp or Ibu was added on top of preloaded serum albumin on MIN6 cells.

Our combined results show that the presence of FAs is a prerequisite for  $\beta$ -cell stimulation by glucose and that

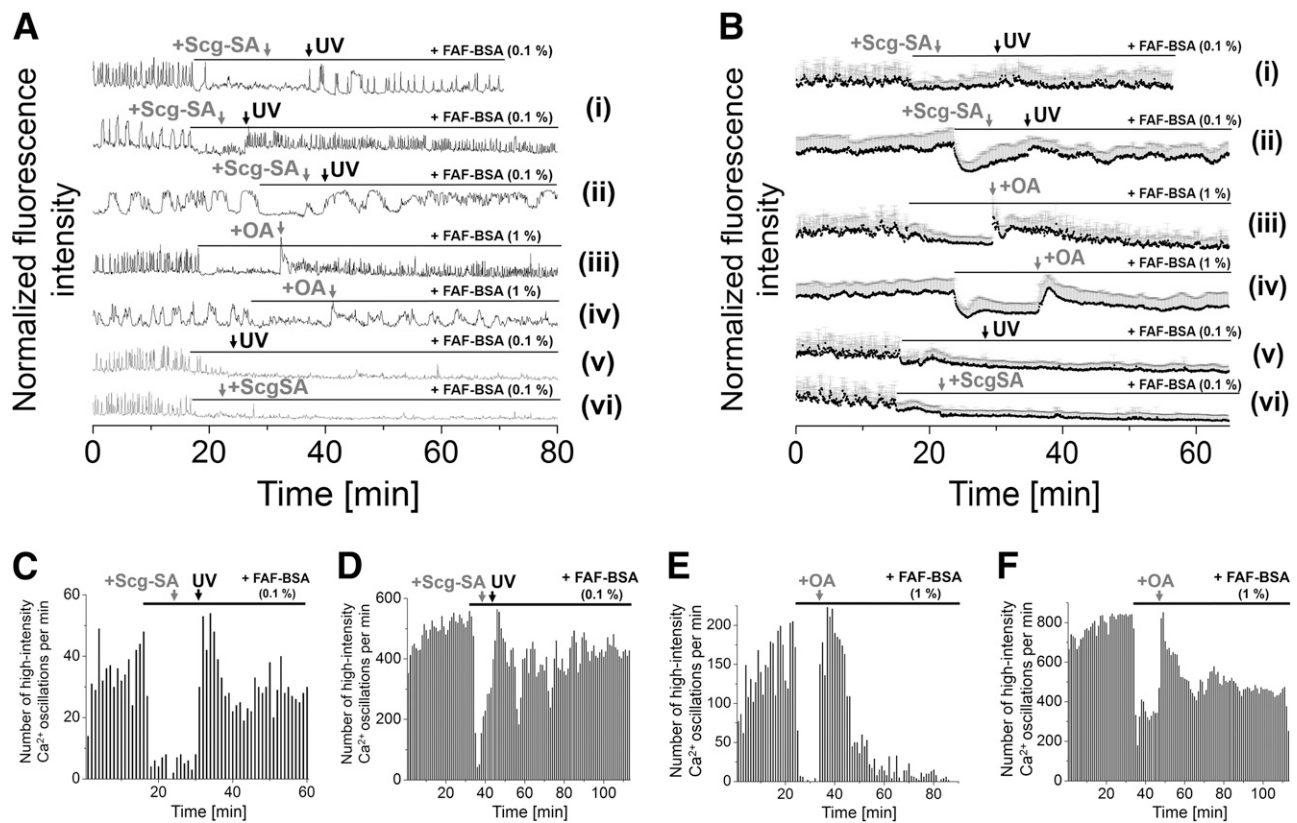


**Figure 6**—Photolysis of coumarin Scg-SA restarts  $[Ca^{2+}]_i$  oscillations that had been terminated by FAF-BSA. *A* and *B*: Representative single (*A*) and averaged (*B*)  $Ca^{2+}$  traces from MIN6 cells and mouse primary  $\beta$ -cells, recorded with the  $Ca^{2+}$  indicator Fluo-4. After FAF-BSA (0.1%)–mediated termination,  $[Ca^{2+}]_i$  oscillations were reconstituted by the photolysis of Scg-SA (200  $\mu$ mol/L,  $\lambda = 375$  nm) or by the addition of OA (200  $\mu$ mol/L) in MIN6 cells (traces i and iii) and mouse primary  $\beta$ -cells (traces ii and iv). Controls demonstrate that without Scg-SA (trace v) or without the UV pulse (trace vi)  $[Ca^{2+}]_i$  oscillations did not resume. *C–F*: Number of detected high-intensity  $[Ca^{2+}]_i$  events within every 60-s interval. Photolysis of Scg-SA (200  $\mu$ mol/L) or addition of OA (200  $\mu$ mol/L, each) restarted  $[Ca^{2+}]_i$  oscillations in MIN6 cells (*C* and *E*) and mouse primary  $\beta$ -cells (*D* and *F*) after the addition of FAF-BSA (0.1%). Shown are the averages of  $n = 14$  MIN6 cells (*B*, trace i, and *C*) and  $n = 30$  MIN6 cells and  $n = 60$  mouse primary  $\beta$ -cells for other experiments. Error bars represent the SD. See Supplementary Fig. 16 for exemplary single  $Ca^{2+}$  traces and Supplementary Fig. 17 for Scg-OA data. Experiments were conducted in the presence of 11 mmol/L glucose.

insulin secretion relies entirely on the presence and maintenance of a basal FA level. The very small and confined volumes of the extracellular space of  $\beta$ -cells, as shown in electron microscopy data (48), might guarantee effective endogenous signaling, since only very low amounts of extracellular signaling factors might be necessary.

To demonstrate that the regulation of solely endogenous FA levels is sufficient to enhance  $[Ca^{2+}]_i$  oscillations in glucose-stimulated  $\beta$ -cells, we artificially elevated FA levels by adding the recombinant lipases PLA<sub>2</sub> or lipoprotein lipase, which immediately translated into increased  $[Ca^{2+}]_i$  oscillations. Further support came from the inhibition of endogenous PLA<sub>2</sub> using MAF and BEL, respectively, which decreased  $[Ca^{2+}]_i$  oscillations and insulin levels. As lipase inhibition reduced  $[Ca^{2+}]_i$  oscillations, endogenous PLA<sub>2</sub> activity seemed to be essential for driving cell responses to glucose. The results further suggest that both external and PM-localized FA pools are essential for  $\beta$ -cell activity, independent of the FA source.

To determine the target of FAs in  $\beta$ -cells, we used the GPR40 antagonist GW1100. It showed an immediate effect on the recovery of  $[Ca^{2+}]_i$  oscillations both when spiked into BSA that was preloaded on MIN6 cells and when added to MIN6 cells. FA-mediated stimulation of GPR40 has been described to stimulate the G $\alpha_q$ -phospholipase C signaling pathway, resulting in an increase of intracellular inositol triphosphate levels and  $Ca^{2+}$  release from endoplasmic reticulum stores. This, in the presence of glucose, leads to the stimulation of L-type calcium channels and insulin release (13). FAs were also described to reduce the voltage-gated K<sup>+</sup> current in  $\beta$ -cells through GPR40, along with protein kinase A activation, leading to increased  $[Ca^{2+}]_i$  and insulin secretion (49). Withdrawal of FAs by the application of FAF-BSA is suspected to interrupt GPR40-mediated activation of L-type calcium channels and GPR40-mediated reduction of K<sup>+</sup> currents and therefore to diminish overall  $[Ca^{2+}]_i$  levels in  $\beta$ -cells, in accordance with the findings of Schnell et al. (12). However, the rapid termination, the fast recovery of  $\beta$ -cell

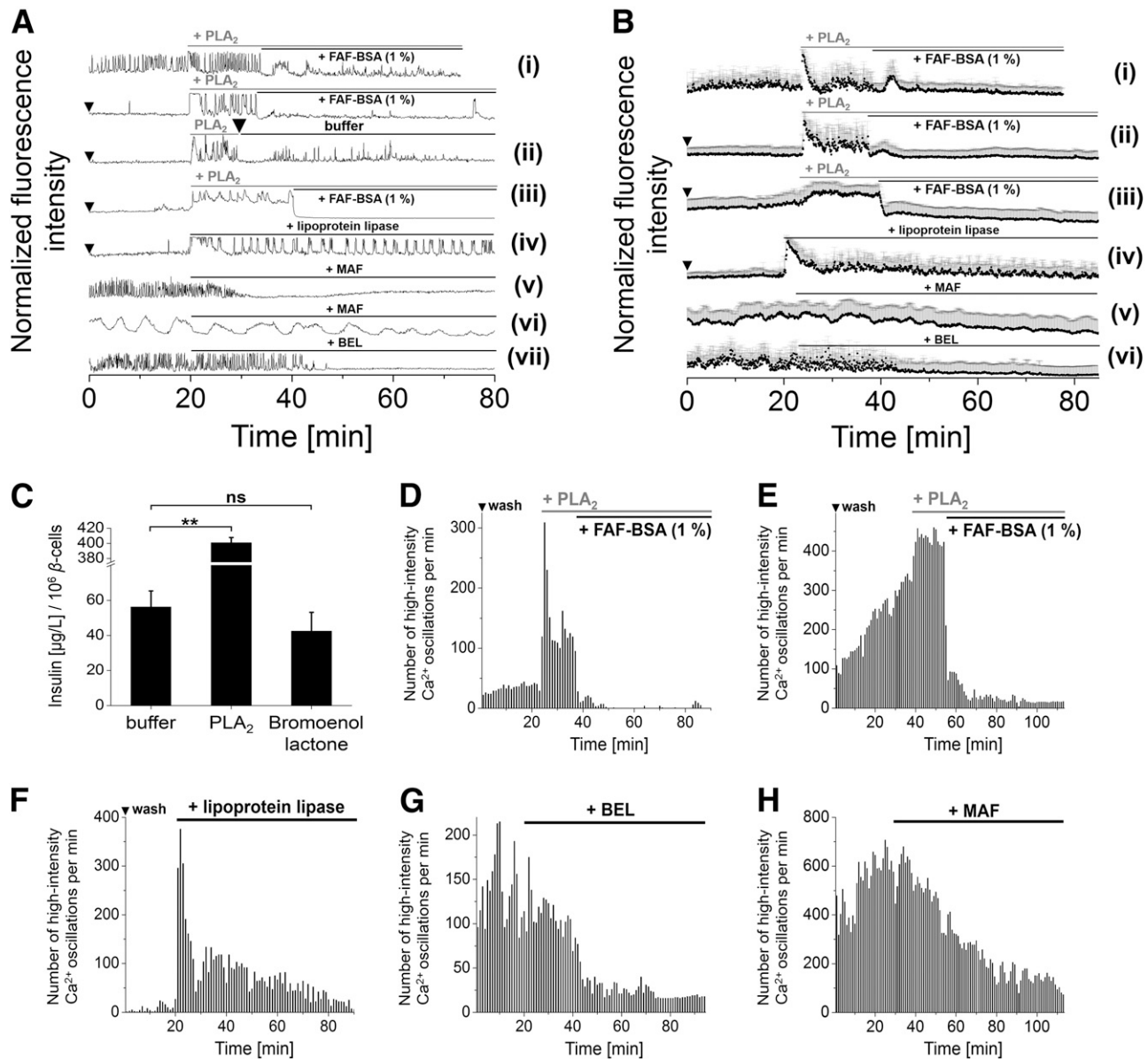


**Figure 7**—Manipulating  $[Ca^{2+}]_i$  oscillations by PLA<sub>2</sub>-mediated FA liberation and BSA-mediated FA depletion. Representative single (A) and averaged (B)  $Ca^{2+}$  traces from MIN6 cells and mouse primary  $\beta$ -cells, recorded with the  $Ca^{2+}$  indicator Fluo-4. Trace i: Addition of PLA<sub>2</sub> (10 units) to MIN6 cells increased  $[Ca^{2+}]_i$  oscillations (trace i), and in prewashed MIN6 cells (trace ii) and mouse primary  $\beta$ -cells (trace iii) (wash indicated by arrows). This stimulation was terminated upon the addition of FAF-BSA (1%) to MIN6 cells (traces i and ii) and mouse primary  $\beta$ -cells (trace iii) or by the exchange of FAF-BSA to buffer (trace ii) (MIN6 cells, 1.5 mL/min). Trace iv: Lipoprotein lipase action (500 units) induced  $[Ca^{2+}]_i$  oscillations in MIN6 cells. PLA<sub>2</sub> inhibitors MAF and BEL (10  $\mu$ mol/L) diminished and finally stopped  $[Ca^{2+}]_i$  oscillations in MIN6 cells (traces v and vii) and mouse primary  $\beta$ -cells (trace vi). **C**: In the presence of PLA<sub>2</sub> (10 units), MIN6 cells increased insulin secretion more than sevenfold over baseline insulin secretion, while the addition of the PLA<sub>2</sub>-inhibitor BEL (10  $\mu$ mol/L) reduced baseline insulin secretion. **D–H**: Number of detected high-intensity  $[Ca^{2+}]_i$  events within every 60-s interval. PLA<sub>2</sub> and lipoprotein lipase increased the number of detected high-intensity  $[Ca^{2+}]_i$  oscillations of MIN6 cells (D and F) and mouse primary  $\beta$ -cells (E) after an initial wash. Induced  $[Ca^{2+}]_i$  oscillations stopped upon the addition of FAF-BSA (D and E) (1%). Inhibition of endogenous PLA<sub>2</sub> by BEL in MIN6 cells and MAF in mouse primary  $\beta$ -cells (G and H) decreased the number of detected high-intensity oscillations. Shown are the averages of  $n = 30$  MIN6 cells and  $n = 60$  mouse primary  $\beta$ -cells. Experiments for the determination of insulin levels were performed in quadruplicate. ns, not significant ( $P > 0.05$ ). \*\* $P < 0.01$ , ANOVA. Error bars represent the SD. See Supplementary Fig. 18 for exemplary single  $Ca^{2+}$  traces. Experiments were conducted in the presence of 11 mmol/L glucose.

activity after addition and replacement of FAF-BSA, and the results from our washing experiments point to additional targets other than GPR40, such as ion channels. Indeed, our recent work on photoswitchable FAs demonstrated a direct

effect of FAs on the activity of voltage-activated and  $K_{ATP}$  channels, and subsequently on glucose-stimulated  $[Ca^{2+}]_i$  oscillations (50). The effect of FAs on ion channels has also been reviewed (49,51).

In conclusion, our combined results imply that intact endogenous signaling is not only important for the synchronization of  $\beta$ -cell populations within pancreatic islets for pulsatile insulin release, but also for the activity at the single  $\beta$ -cell level. Our findings have implications for the general understanding of the regulation of  $\beta$ -cell activity and insulin secretion. In future studies, the impact of drugs that have an affinity for serum albumin on insulin secretion as well as the nutritional state of the organism should be considered. Displacement of anti-inflammatory drugs by FAs and vice versa from albumin binding sites, particularly compounds with low free fractions in plasma, may also be of pharmacokinetic significance. Nutrition- or drug-induced changes of FA levels in blood might have direct effects on insulin secretion.

**Acknowledgments.** The authors thank Rainer Müller (European Molecular Biology Laboratory [EMBL]) and Felix Hoelmann (EMBL) for providing the Scg-SA and Scg-OA and Madeleine Schultz (EMBL) for critical reading of the manuscript. The authors also thank Alexander Aulehla (EMBL) for providing mice for islet isolation.

**Funding.** This research was supported by Deutsche Forschungsgemeinschaft Transregio 83 and 186 (C.S.). D.A.Y. received an Institute of Organic Chemistry and Biochemistry installation grant.

**Duality of Interest.** No potential conflicts of interest relevant to this article were reported.

**Author Contributions.** S.H. designed the research; performed the experiments; analyzed the data; and wrote, reviewed, and edited the manuscript. K.K. performed the experiments, analyzed the data, and reviewed and edited the manuscript. P.P. analyzed the data and reviewed and edited the manuscript. D.A.Y. and C.S. designed the research and wrote, reviewed, and edited the manuscript. C.S. is the guarantor of this work and, as such, had full access to all the data in the study and takes responsibility for the integrity of the data and the accuracy of the data analysis.

## References

- Santos RM, Rosario LM, Nadal A, Garcia-Sancho J, Soria B, Valdeolmillos M. Widespread synchronous  $[Ca^{2+}]_i$  oscillations due to bursting electrical activity in single pancreatic islets. *Pflugers Arch* 1991;418:417–422
- Paolisso G, Sgambato S, Torella R, et al. Pulsatile insulin delivery is more efficient than continuous infusion in modulating islet cell function in normal subjects and patients with type 1 diabetes. *J Clin Endocrinol Metab* 1988;66:1220–1226
- Ravier MA, Sehlin J, Henquin JC. Disorganization of cytoplasmic  $Ca^{2+}$  oscillations and pulsatile insulin secretion in islets from ob/ob mice. *Diabetologia* 2002;45:1154–1163
- Calabrese A, Zhang M, Serre-Beinier V, et al. Connexin 36 controls synchronization of  $Ca^{2+}$  oscillations and insulin secretion in MIN6 cells. *Diabetes* 2003;52:417–424
- Tengholm A, Gylfe E. Oscillatory control of insulin secretion. *Mol Cell Endocrinol* 2009;297:58–72
- Braun M, Ramracheya R, Bengtsson M, et al. Gamma-aminobutyric acid (GABA) is an autocrine excitatory transmitter in human pancreatic beta-cells. *Diabetes* 2010;59:1694–1701
- Wang ZL, Bennet WM, Wang RM, Gbatei MA, Bloom SR. Evidence of a paracrine role of neuropeptide-Y in the regulation of insulin release from pancreatic islets of normal and dexamethasone-treated rats. *Endocrinology* 1994;135:200–206
- Grapengiesser E, Dansk H, Hellman B. External ATP triggers  $Ca^{2+}$  signals suited for synchronization of pancreatic beta-cells. *J Endocrinol* 2005;185:69–79
- Itoh Y, Kawamata Y, Harada M, et al. Free fatty acids regulate insulin secretion from pancreatic beta cells through GPR40. *Nature* 2003;422:173–176
- Briscoe CP, Tadayon M, Andrews JL, et al. The orphan G protein-coupled receptor GPR40 is activated by medium and long chain fatty acids. *J Biol Chem* 2003;278:11303–11311
- Kotarsky K, Nilsson NE, Flodgren E, Owman C, Olde B. A human cell surface receptor activated by free fatty acids and thiazolidinedione drugs. *Biochem Biophys Res Commun* 2003;301:406–410
- Schnell S, Schaefer M, Schöfl C. Free fatty acids increase cytosolic free calcium and stimulate insulin secretion from  $\beta$ -cells through activation of GPR40. *Mol Cell Endocrinol* 2007;263:173–180
- Shapiro H, Shachar S, Sekler I, Hershinkel M, Walker MD. Role of GPR40 in fatty acid action on the  $\beta$  cell line INS-1E. *Biochem Biophys Res Commun* 2005;335:97–104
- Alquier T, Peyot M-L, Latour MG, et al. Deletion of GPR40 impairs glucose-induced insulin secretion in vivo in mice without affecting intracellular fuel metabolism in islets. *Diabetes* 2009;58:2607–2615
- Nagasumi K, Esaki R, Iwachidow K, et al. Overexpression of GPR40 in pancreatic  $\beta$ -cells augments glucose-stimulated insulin secretion and improves glucose tolerance in normal and diabetic mice. *Diabetes* 2009;58:1067–1076
- Nadler A, Yushchenko DA, Müller R, et al. Exclusive photorelease of signalling lipids at the plasma membrane. *Nat Commun* 2015;6:10056
- Komatsu M, Yajima H, Yamada S, et al. Augmentation of  $Ca^{2+}$ -stimulated insulin release by glucose and long-chain fatty acids in rat pancreatic islets: free fatty acids mimic ATP-sensitive  $K^+$  channel-independent insulinotropic action of glucose. *Diabetes* 1999;48:1543–1549
- Crespin SR, Greenough WB III, Steinberg D. Stimulation of insulin secretion by long-chain free fatty acids. A direct pancreatic effect. *J Clin Invest* 1973;52:1979–1984
- Dobbins RL, Chester MW, Daniels MB, McGarry JD, Stein DT. Circulating fatty acids are essential for efficient glucose-stimulated insulin secretion after prolonged fasting in humans. *Diabetes* 1998;47:1613–1618
- Hosokawa H, Corkey BE, Leahy JL. Beta-cell hypersensitivity to glucose following 24-h exposure of rat islets to fatty acids. *Diabetologia* 1997;40:392–397
- Boden G, Chen X, Iqbal N. Acute lowering of plasma fatty acids lowers basal insulin secretion in diabetic and nondiabetic subjects. *Diabetes* 1998;47:1609–1612
- Stein DT, Esser V, Stevenson BE, et al. Essentiality of circulating fatty acids for glucose-stimulated insulin secretion in the fasted rat. *J Clin Invest* 1996;97:2728–2735
- Nolan CJ, Madiraju MSR, Delghingaro-Augusto V, Peyot M-L, Prentki M. Fatty acid signaling in the  $\beta$ -cell and insulin secretion. *Diabetes* 2006;55(Suppl. 2):S16–S23
- Miyazaki J, Araki K, Yamato E, et al. Establishment of a pancreatic  $\beta$  cell line that retains glucose-inducible insulin secretion: special reference to expression of glucose transporter isoforms. *Endocrinology* 1990;127:126–132
- Ravier MA, Rutter GA. Isolation and culture of mouse pancreatic islets for ex vivo imaging studies with trappable or recombinant fluorescent probes. *Methods Mol Biol* 2010;633:171–184
- Schindelin J, Arganda-Carreras I, Frise E, et al. Fiji: an open-source platform for biological-image analysis. *Nat Methods* 2012;9:676–682
- Greenspan P, Fowler SD. Spectrofluorometric studies of the lipid probe, Nile red. *J Lipid Res* 1985;26:781–789
- Clark J, Anderson KE, Juvin V, et al. Quantification of PtdInsP3 molecular species in cells and tissues by mass spectrometry. *Nat Methods* 2011;8:267–272
- Yao C-H, Liu G-Y, Yang K, Gross RW, Patti GJ. Inaccurate quantitation of palmitate in metabolomics and isotope tracer studies due to plastics. *Metabolomics* 2016;12:143–149
- Ishihara H, Asano T, Tsukuda K, et al. Pancreatic beta cell line MIN6 exhibits characteristics of glucose metabolism and glucose-stimulated insulin secretion similar to those of normal islets. *Diabetologia* 1993;36:1139–1145
- Gilon P, Shepherd RM, Henquin JC. Oscillations of secretion driven by oscillations of cytoplasmic  $Ca^{2+}$  as evidences in single pancreatic islets. *J Biol Chem* 1993;268:22265–22268

32. Bergsten P. Slow and fast oscillations of cytoplasmic  $\text{Ca}^{2+}$  in pancreatic islets correspond to pulsatile insulin release. *Am J Physiol* 1995;268:E282–E287
33. Jonas J-C, Gilon P, Henquin JC. Temporal and quantitative correlations between insulin secretion and stably elevated or oscillatory cytoplasmic  $\text{Ca}^{2+}$  in mouse pancreatic  $\beta$ -cells. *Diabetes* 1998;47:1266–1273
34. Gee KR, Brown KA, Chen W-NU, Bishop-Stewart J, Gray D, Johnson I. Chemical and physiological characterization of fluo-4  $\text{Ca}^{2+}$ -indicator dyes. *Cell Calcium* 2000;27:97–106
35. McMenemy RH, Oncley JL. The specific binding of L-tryptophan to serum albumin. *J Biol Chem* 1958;233:1436–1447
36. Whittam JB, Crooks MJ, Brown KF, Pedersen PV. Binding of nonsteroidal anti-inflammatory agents to proteins—I. Ibuprofen-serum albumin interaction. *Biochem Pharmacol* 1979;28:675–678
37. Briscoe CP, Peat AJ, McKeown SC, et al. Pharmacological regulation of insulin secretion in MIN6 cells through the fatty acid receptor GPR40: identification of agonist and antagonist small molecules. *Br J Pharmacol* 2006;148:619–628
38. Black SL, Stanley WA, Filipp FV, et al. Probing lipid- and drug-binding domains with fluorescent dyes. *Bioorg Med Chem* 2008;16:1162–1173
39. Burke JE, Dennis EA. Phospholipase A2 structure/function, mechanism, and signaling. *J Lipid Res* 2009;50(Suppl.):S237–S242
40. Mead JR, Irvine SA, Ramji DP. Lipoprotein lipase: structure, function, regulation, and role in disease. *J Mol Med (Berl)* 2002;80:753–769
41. Newgard CB, McGarry JD. Metabolic coupling factors in pancreatic  $\beta$ -cell signal transduction. *Annu Rev Biochem* 1995;64:689–719
42. Torres N, Noriega L, Tovar AR. Nutrient modulation of insulin secretion. *Vitam Horm* 2009;80:217–244
43. Sacco F, Humphrey SJ, Cox J, et al. Glucose-regulated and drug-perturbed phosphoproteome reveals molecular mechanisms controlling insulin secretion. *Nat Commun* 2016;7:13250
44. Ashbrook JD, Spector AA, Santos EC, Fletcher JE. Long chain fatty acid binding to human plasma albumin. *J Biol Chem* 1975;250:2333–2338
45. Ashbrook JD, Spector AA, Fletcher JE. Medium chain fatty acid binding to human plasma albumin. *J Biol Chem* 1972;247:7038–7042
46. Kober A, Sjöholm I. The binding sites on human serum albumin for some nonsteroidal antiinflammatory drugs. *Mol Pharmacol* 1980;18:421–426
47. Hamilton JA, Era S, Bhamidipati SP, Reed RG. Locations of the three primary binding sites for long-chain fatty acids on bovine serum albumin. *Proc Natl Acad Sci U S A* 1991;88:2051–2054
48. Longnecker DS. Anatomy and histology of the pancreas [Internet], 2014. Available from <https://www.pancreapedia.org/reviews/anatomy-and-histology-of-pancreas>. Accessed 17 January 2017
49. Feng DD, Luo Z, Roh SG, et al. Reduction in voltage-gated  $\text{K}^{+}$  currents in primary cultured rat pancreatic  $\beta$ -cells by linoleic acids. *Endocrinology* 2006;147:674–682
50. Frank JA, Yushchenko DA, Fine NHF, et al. Optical control of GPR40 signalling in pancreatic  $\beta$ -cells. *Chem Sci (Camb)* 2017;8:7604–7610
51. Jacobson DA, Weber CR, Bao S, Turk J, Philipson LH. Modulation of the pancreatic islet beta-cell-delayed rectifier potassium channel  $\text{Kv}2.1$  by the polyunsaturated fatty acid arachidonate. *J Biol Chem* 2007;282:7442–7449